


Berry curvature for magnetoelastic wavesAkihiro Okamoto,¹ Shuichi Murakami ,¹ and Karin Everschor-Sitte ²¹*Department of Physics, Tokyo Institute of Technology, 2-12-1 Ookayama, Meguro-ku, Tokyo 152-8551, Japan*²*Institute of Physics, Johannes Gutenberg-Universität Mainz, 55128, Mainz, Germany*

(Received 6 October 2019; revised manuscript received 7 February 2020; accepted 7 February 2020; published 25 February 2020)

The Berry curvature for magnons in ferromagnetic films gives rise to new phenomena such as thermal Hall effect and a shift of a magnon wave packet at the reflection at the edge of the magnetic film. In this paper, we calculate the Berry curvature of magnetoelastic waves in ferromagnets. In order to calculate the Berry curvature, we first formulate the eigenvalue equation into a Hermitian form from the dynamical equation of motion. We find that the Berry curvature of the magnetoelastic waves shows a peak at the crossing point of the dispersions of magnons and elastic waves, and its peak value is dependent on the hybridization gap at the crossing point. In addition, the behavior of the Berry curvature in the long-wavelength limit changes drastically by the magnetoelastic interaction. We calculate the effect of dipolar interactions in a magnetic film on the Berry curvature, and we find a sign change by increasing the film thickness. The effect of the Berry curvature may be detected by measuring the shift of a wave packet for magnetoelastic waves at a reflection at the edge of a magnet and we find that a shift shows an abrupt change when the wave vector changes across the crossing point.

DOI: [10.1103/PhysRevB.101.064424](https://doi.org/10.1103/PhysRevB.101.064424)**I. INTRODUCTION**

Spin waves in ferromagnets hybridize with phonons via the magnetoelastic interaction. Such coupled waves are called magnetoelastic waves and were theoretically predicted by Kittel [1] and Akhiezer [2] and extended by Schlömann [3]. Subsequently they were observed experimentally [4–7]. Since then, they have been studied intensively together with the progress of the observation techniques of spin waves. Recently, the dispersion of the magnetostatic wave was observed directly by spin-wave tomography, which clearly showed the effect of the magnetoelastic coupling [8]. Moreover, new phenomena on the magnetoelastic wave have been predicted, such as the spatial magnetization dynamics in magnetic thin films induced by a laser [9] as well as characteristics of transmittance between the nonmagnetic transducer and the magnetic material [10,11]. In addition, experiments have shown that the spin Seebeck effect is enhanced at the crossing point of the magnon and phonon dispersions [12]. Moreover, the effect of the hybridization between the magnon and the phonon branches appears as the gap in the Bose-Einstein magnon states [13].

In this paper, we study the Berry curvature of the magnetoelastic waves. Berry curvature is a differential-geometric quantity and can be expressed in terms of Bloch wave functions. Its effect is studied in Hall effects, in the shift of a wave packet, and even in various topological phases for various particles such as photons [14–18]. One of the interactions inducing a nonzero Berry curvature of magnons is the dipolar interaction [19,20]. When we include only the dipolar interaction in a ferromagnetic film the Berry curvature is always positive [19,20]. In the previous paper [21], we focus on the Berry curvature of magnons with dipole and exchange interactions in a ferromagnetic film. When we incorporate

the exchange interaction, the Berry curvature changes its sign at the crossover between the dipolar interaction and the exchange interaction. Besides, the Berry curvature shows a peak at the crossing point of dispersions between two eigenmodes due to the hybridization. It is well known that the Berry curvature is affected by hybridization of different types of waves. For example, the magnetoelastic interaction hybridizes the magnon and the elastic wave and alters their dispersions [1–3]. Therefore it seems natural that the magnetoelastic wave shows nonzero Berry curvature. Recently, the emergence of topological bands due to the hybridization between magnons and phonons has been reported. The magnetoelastic interaction between the magnetization direction and the elastic strain [1] leads to topological bands separated by a hybridization gap, as has been discussed in a lattice model in Ref. [22]. In Ref. [23], it is shown that another type of a magnetoelastic coupling, coming from the DM interaction, leads to topological bands. In this paper, we show emergence of topological bands due to the magnetoelastic interaction in a continuum model [1] without the DM interaction. This theory based on a continuum model is appropriate for describing magnons with a wavelength much longer than the lattice constant. This wavelength regime has been well studied in experiments [4–7], where the lattice structure of the system does not so much affect the physics.

In the following section, we calculate the Berry curvature of the magnetoelastic wave. Calculation of the Berry curvature requires Hermiticity of the eigenvalue problem. However, the eigenvalue equation derived from the dynamical equation of motion is non-Hermitian. In this paper, we introduce a new approach to formulate the eigenvalue equation in a Hermitian form to calculate the Berry curvature of the magnetoelastic wave. The Berry curvature is enhanced at the crossing point of the dispersions of the magnon and the elastic wave, even when

the dipolar interaction is already saturated in contrast to the Berry curvature of the magnon. In addition, we find that the behavior of Berry curvature in the vicinity of $k \rightarrow 0$ becomes nonzero due to the magnetoelastic interaction, because the magnetoelastic interaction affects on their dispersions even in the region of small k . In the last part of this paper, we calculate the shift of the wave packet of the magnetoelastic wave at the reflection at the edge of the magnet. We find that the shift appears abruptly when the wave number of the incident wave becomes larger than the crossing point when the coupling is small and that the behavior of the shift is dependent on the strength of the magnetoelastic coupling.

This paper is organized as follows. In Sec. II, we formulate a Hermitian eigenvalue problem from the equations of motion of magnons and elastic waves. In Secs. III and IV, we calculate the Berry curvature of magnetoelastic waves and shifts by a reflection. We summarize the paper in Sec. V.

II. FORMULATION OF EIGENVALUE EQUATION

Here, we present the eigenvalue equation for magnons and elastic waves in a ferromagnet with a magnetoelastic coupling. Because the eigenvalue equation is not of the Hermitian form, formulation of the Berry curvature is not straightforward. For example, in phonon systems, the effective Hamiltonian derived from the dynamical equation is not Hermitian [24–26]. Therefore, in Refs. [24,25], left- and right-eigenvalue problems for the phonon systems are formulated and their eigenvectors are used for calculations of the Berry curvature to derive the thermal Hall conductivity. In this paper, we use a different approach to calculate the Berry curvature for the magnon and the elastic wave.

We first formulate an eigenvalue equation for magnons and elastic waves in a Hermitian form. We consider an eigenvalue equation

$$i \frac{\partial}{\partial t} \mathbf{x}_k = H_{\text{eff}} \mathbf{x}_k, \quad (1)$$

where \mathbf{x}_k is the eigenvector, \mathbf{k} is the wave vector, and H_{eff} is an operator which is not necessarily Hermitian. We call H_{eff} an effective Hamiltonian. Let \mathbf{x}_k be proportional to $e^{-i\omega t}$, where ω is an eigenfrequency. Then we get

$$\omega \mathbf{x}_k = H_{\text{eff}} \mathbf{x}_k. \quad (2)$$

In the present problem of the magnetoelastic wave, H_{eff} is not Hermitian. Here, let us assume that there exists a Hermitian matrix γ which makes $\tilde{H}_{\text{eff}} \equiv \gamma H_{\text{eff}}$ also Hermitian. We rewrite Eq. (2) into the following form:

$$\omega \gamma \mathbf{x}_k = \gamma H_{\text{eff}} \mathbf{x}_k. \quad (3)$$

We can then show that $\mathbf{x}_k^\dagger \gamma \mathbf{x}_k$ is conserved:

$$\frac{\partial}{\partial t} (\mathbf{x}_k^\dagger \gamma \mathbf{x}_k) = -i \mathbf{x}_k^\dagger H_{\text{eff}}^\dagger \gamma \mathbf{x}_k + i \mathbf{x}_k^\dagger \gamma H_{\text{eff}} \mathbf{x}_k = 0. \quad (4)$$

We can then take a normalization condition as

$$\mathbf{x}_k^\dagger \gamma \mathbf{x}_k = 1. \quad (5)$$

We apply this formalism to the magnetoelastic wave in the following section.

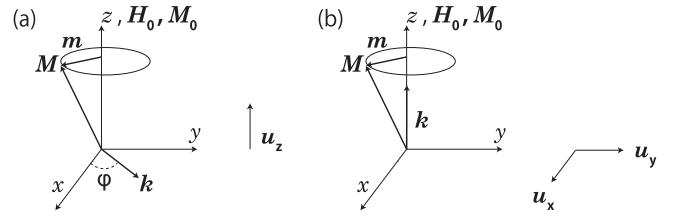


FIG. 1. Schematic illustration of the magnetoelastic waves for (a) the wave vector \mathbf{k} perpendicular to the saturation magnetization \mathbf{M}_0 , as discussed in main text (b) $\mathbf{k} \parallel \mathbf{M}_0$, see Appendix A.

A. Magnetoelastic wave

Derivation of the eigenvalues for magnetoelastic waves as a classical problem is well studied [1–3,27–29]. In the presence of the magnetoelastic coupling the dispersions are dependent on the orientations of the wave vector and the magnetization [3,27,28]. We consider a ferromagnet with the saturation magnetization \mathbf{M}_0 and the applied magnetic field \mathbf{H}_0 both along the z direction. Then the magnon is described by a vector \mathbf{m} in the xy plane. We take into account the Zeeman interaction, the exchange interaction, the dipolar field, and the magnetoelastic interaction. Here we assume the system to be elastically isotropic and neglect dissipation in the system. The dynamical equation of magnons and elastic waves with magnetoelastic interaction in three dimensions are written in Appendix A. We consider magnetoelastic waves in two geometries; the wave vector perpendicular to the magnetization in the following sector, and that parallel to the magnetization in Appendix A.

When the wave vector is perpendicular to the magnetization and is in the xy plane, the dipole field is not negligible and its effect appears in the magnon dispersion [28]. In that situation, the dynamical equations are written as

$$-i\omega m_x = -\Omega_0 m_y - \omega_M \sin \varphi (\cos \varphi m_x + \sin \varphi m_y) - igB_2 k_y u_z, \quad (6a)$$

$$-i\omega m_y = \Omega_0 m_x + \omega_M \cos \varphi (\cos \varphi m_x + \sin \varphi m_y) + igB_2 k_x u_z, \quad (6b)$$

$$-\rho_0 \omega^2 u_x = -c_{44} k^2 u_x - (c_{44} + c_{12}) k_x \mathbf{k} \cdot \mathbf{u}, \quad (6c)$$

$$-\rho_0 \omega^2 u_y = -c_{44} k^2 u_y - (c_{44} + c_{12}) k_y \mathbf{k} \cdot \mathbf{u}, \quad (6d)$$

$$-\rho_0 \omega^2 u_z = -c_{44} k^2 u_z + i \frac{gB_2}{\omega_M} (k_x m_x + k_y m_y), \quad (6e)$$

where $\omega_M = gM_0$, g is the gyromagnetic ratio, \mathbf{u} is the displacement vector, c_{12} and c_{44} are elastic modules whose expressions are written in Appendix A, B_2 is the magnetoelastic constant, ρ_0 is the equilibrium mass density, Ω_0 includes only the Zeeman energy and the exchange interaction such as $\Omega_0 = \omega_H + \omega_M \alpha k^2$, $\omega_H = gH_0$ and α is the exchange constant as in Ref. [30], and φ is the azimuthal angle between the x axis and the wave vector \mathbf{k} within the xy plane [Fig. 1 (a)]. In the dynamical equations, \mathbf{m} and u_z couple with each other whereas u_x and u_y are decoupled. Thus we regard $\mathbf{x} = (m_x, m_y, u_z, u_x)$ as the eigenvector in Eq. (1), and the effective Hamiltonian

H_{eff} is written as

$$H_{\text{eff}} = \begin{pmatrix} -i\omega_M \sin \varphi \cos \varphi & -i(\Omega_0 + \omega_M \sin^2 \varphi) & 0 & gB_2k_y \\ i(\Omega_0 + \omega_M \cos^2 \varphi) & i\omega_M \sin \varphi \cos \varphi & 0 & -gB_2k_x \\ -\frac{gB_2}{\rho_0\omega_M}k_x & -\frac{gB_2}{\rho_0\omega_M}k_y & 0 & -ic_{44}k^2/\rho_0 \\ 0 & 0 & i & 0 \end{pmatrix}. \quad (7)$$

We find the Hermitian matrix γ which makes $\tilde{H}_{\text{eff}} \equiv \gamma H_{\text{eff}}$ Hermitian is given by

$$\gamma = \begin{pmatrix} 0 & -i & 0 & 0 \\ i & 0 & 0 & 0 \\ 0 & 0 & 0 & -i\rho_0\omega_M \\ 0 & 0 & i\rho_0\omega_M & 0 \end{pmatrix}. \quad (8)$$

Next, we calculate dispersion relations using the Hermitian matrix \tilde{H}_{eff} defined as $\tilde{H}_{\text{eff}} = \gamma H_{\text{eff}}$. This Hamiltonian is written as

$$\tilde{H}_{\text{eff}} = \begin{pmatrix} \Omega_0 + \omega_M \cos^2 \varphi & \omega_M \sin \varphi \cos \varphi & 0 & igB_2k \cos \varphi \\ \omega_M \sin \varphi \cos \varphi & \Omega_0 + \omega_M \sin^2 \varphi & 0 & igB_2k \sin \varphi \\ 0 & 0 & \omega_M \rho_0 & 0 \\ -igB_2k \cos \varphi & -igB_2k \sin \varphi & 0 & \omega_M c_{44}k^2 \end{pmatrix}. \quad (9)$$

Then, the eigenvalue equation (3) for the eigenvector \mathbf{x}_k is written as

$$\begin{pmatrix} \Omega_0 + \omega_M \cos^2 \varphi & \omega_M \sin \varphi \cos \varphi + i\omega & 0 & igB_2k \cos \varphi \\ \omega_M \sin \varphi \cos \varphi - i\omega & \Omega_0 + \omega_M \sin^2 \varphi & 0 & igB_2k \sin \varphi \\ 0 & 0 & \omega_M \rho_0 & i\rho_0\omega_M \omega \\ -igB_2k \cos \varphi & -igB_2k \sin \varphi & -i\rho_0\omega_M \omega & \omega_M c_{44}k^2 \end{pmatrix} \begin{pmatrix} m_x \\ m_y \\ \dot{u}_z \\ u_z \end{pmatrix} = \mathbf{0}. \quad (10)$$

The eigenvalue ω is derived from the above equation as

$$(\omega^2 - \omega_{\text{mag}}^2)(\omega^2 - \omega_{\text{ela}}^2) = \frac{g^2 \Omega_0 B_2^2 k^2}{\rho_0 \omega_M}, \quad (11)$$

where we define $\omega_{\text{mag}}^2 = \Omega_0(\Omega_0 + \omega_M)$, and $\omega_{\text{ela}}^2 = c_{44}k^2/\rho_0$. This dispersion relation is the same as that obtained in Ref. [3]. The right-hand side of Eq. (11) represents the magnetoelastic interaction. When the magnetoelastic coupling is absent, the dispersion of phonons $\omega = \omega_{\text{ela}}$ and that of magnons $\omega = \omega_{\text{mag}}$ cross at the wave vector $k^* \equiv \sqrt{\frac{\rho_0}{c_{44}}} \omega_{\text{mag}}$ (Appendix C). The magnetoelastic interaction makes this crossing into an avoided crossing. The norm $\mathbf{x}_k^\dagger \gamma \mathbf{x}_k$ is written as

$$\begin{aligned} \mathbf{x}_k^\dagger \gamma \mathbf{x}_k &= i(-m_x^* m_y + m_y^* m_x) + 2\rho_0 \omega \omega_M |u_z|^2 \\ &= 4 \frac{\omega_M}{\omega} (\varepsilon_{\text{mag}} + \varepsilon_{\text{ela}}), \end{aligned} \quad (12)$$

where ε_{mag} and ε_{ela} are the energy densities of the magnon [31,32] and that of the elastic wave [33,34], respectively. From Eq. (12), $\mathbf{x}_k^\dagger \gamma \mathbf{x}_k$ is proportional to the total energy density, and is a constant of motion due to the translational invariance in time. In fact, the form of the matrix γ in Eq. (8) is found so as to make $\mathbf{x}_k^\dagger \gamma \mathbf{x}_k$ to be proportional to the total energy density.

Recently the eigenvalue problem of magnetoelastic waves in a ferromagnet has been studied in Ref. [35], and we here compare our results with Ref. [35]. In the main text of Ref. [35], spins and phonons are treated quantum-mechanically, using the Green function method. If we take the classical limit: spin $S \rightarrow \infty$, the results corresponds to our classical results. In the Appendix of Ref. [35] the classical equation of motions are discussed with an approximation of

limiting the number of phonon modes into one. Apart from this approximation, their classical result is the same as ours.

III. BERRY CURVATURE OF THE MAGNETOELASTIC WAVES

In the previous section, we formulated the generalized Hermitian eigenvalue equation for the magnetoelastic waves. In this section, we calculate the Berry curvature of the magnetoelastic wave. The Berry curvature for the present classical eigenvalue problem is defined as

$$\Omega_{n,z}(\mathbf{k}) = i\epsilon_{ij} \frac{\partial \mathbf{x}_{n,\mathbf{k}}^\dagger}{\partial k_i} \gamma \frac{\partial \mathbf{x}_{n,\mathbf{k}}}{\partial k_j}. \quad (13)$$

The derivation of the above equation is written in Appendix B, by formulating a semiclassical equation of motion. Here, we note that the definition of $\Omega_{n,z}(\mathbf{k})$ in Eq. (13) needs the matrix γ to guarantee the gauge invariance for the Berry curvature; under the gauge transformation $\mathbf{x}_k \Rightarrow \tilde{\mathbf{x}}_k = e^{i\Theta_k} \mathbf{x}_k$ (Θ_k : real), the Berry curvature is invariant (see Appendix B).

Next, we calculate the eigenfrequency at the crossing point of the dispersions of magnons and elastic waves, because the Berry curvature is expected to be enhanced there. From Eq. (11), we obtain the eigenfrequencies

$$\omega_{\pm}^2 = \frac{\omega_{\text{mag}}^2 + \omega_{\text{ela}}^2}{2} \pm \sqrt{\left(\frac{\omega_{\text{mag}}^2 - \omega_{\text{ela}}^2}{2}\right)^2 + (\zeta k)^2}, \quad (14)$$

where $\zeta = \sqrt{g\Omega_0 B_2^2 / \rho_0 M_0}$. At the crossing point $k = k^*$, the frequencies of the magnon and the elastic wave are the same.

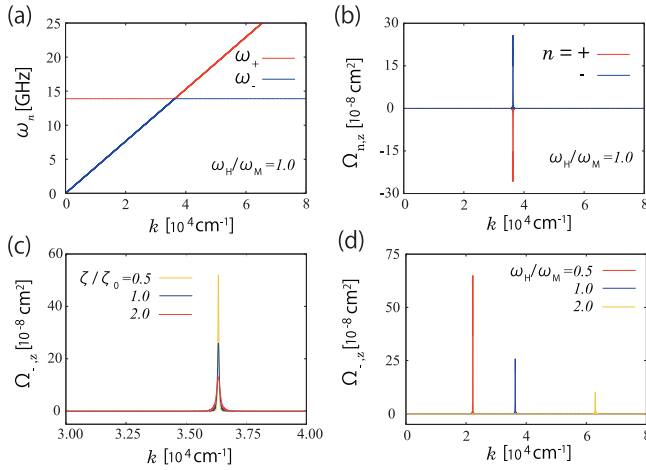


FIG. 2. (a) Dispersion of the magnetoelastic wave, and (b) its Berry curvature for $\omega_H/\omega_M = 1.0$. Berry curvature of ω_- for (c) $\zeta/\zeta_0 = 0.5, 1.0, 2.0$ with $\omega_H/\omega_M = 1.0$, and (d) $\omega_H/\omega_M = 0.5, 1.0, 2.0$ with $\zeta/\zeta_0 = 1.0$.

Let $\tilde{\omega}$ denote the frequency of these waves without coupling:

$$\omega_{\text{mag}}(k^*) = \omega_{\text{ela}}(k^*) = \tilde{\omega}. \quad (15)$$

From Eq. (14), the eigenfrequencies at the crossing point and a hybridization gap $\Delta\omega$ is written as

$$\omega_{\pm} = \tilde{\omega} \pm \frac{1}{2} \Delta\omega, \quad \Delta\omega \equiv \frac{\zeta k^*}{\tilde{\omega}}. \quad (16)$$

In addition, when $k \ll k^*$, the dispersion for the ω_+ branch is written as

$$\omega_+^2 \approx \omega_0^2 + \omega_M(2\omega_H + \omega_M)\alpha k^2 + \left(\frac{\zeta k}{\omega_0}\right)^2, \quad (17)$$

where $\omega_0^2 = \omega_H(\omega_H + \omega_M)$. The first term is the dispersion of the magnetostatic spin wave. The second and third terms are the contributions from the exchange and the elastic interactions, respectively. The dispersion for the ω_- branch is written as

$$\omega_-^2 \approx \omega_{\text{ela}}^2 - \left(\frac{\zeta k}{\omega_0}\right)^2 \equiv c'^2 k^2, \quad (18)$$

where $c' = \sqrt{c_{44}/\rho_0 - \zeta^2/\omega_0^2}$.

In the following, we calculate the Berry curvature in the cases with weak and strong magnetoelastic coupling. We classify the cases of the weak or strong magnetoelastic coupling according to whether the magnetoelastic constant and wave number satisfy $\zeta k^* \ll \omega_0$ or not in the dispersions.

A. Weak magnetoelastic coupling

When the magnetoelastic interaction is weak, the hybridization gap $\Delta\omega$ becomes small. Therefore, the Berry curvature at the crossing point of the dispersions is expected to become large, as is similar to the previous result on the hybridization gap between magnetostatic modes in a ferromagnetic slab [21]. Here we only focus on the wave number close to the crossing point of the dispersions. We illustrate results of our numerical calculations for the magnetoelastic wave in Fig. 2. We take the parameter values $M_0 = 278.5$ G, $c_{44} = 7.6 \times 10^{11}$ erg/cm³, $\rho_0 = 5.2$ g/cm³, and $B_2 = 6.7 \times$

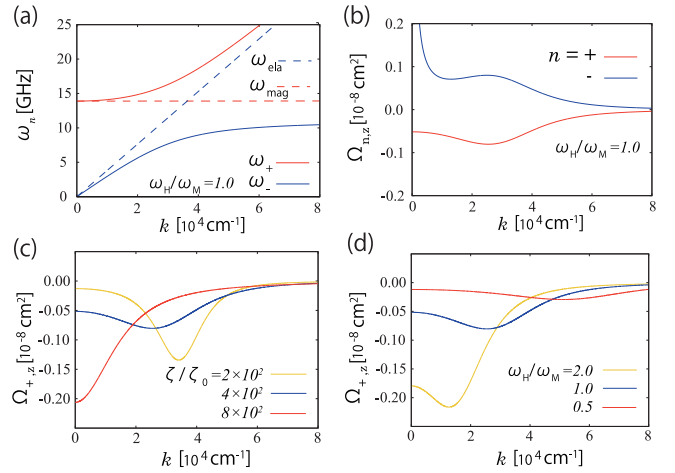


FIG. 3. (a) Dispersion of the magnetoelastic wave, and (b) its Berry curvature for $\omega_H/\omega_M = 1.0$ with $\zeta = 4 \times 10^2 \zeta_0$. Berry curvature of ω_+ for (c) $\zeta = 2, 4, 8 \times 10^2 \zeta_0$ with $\omega_H/\omega_M = 1.0$, and (d) $\omega_H/\omega_M = 0.5, 1.0, 2.0$ with $\zeta = 4 \times 10^2 \zeta_0$.

10^6 erg/cm³ for YIG from Refs. [28,36]. From these parameters, the third term in Eq. (17) is much smaller than the first term. The second term in Eq. (17) is also smaller than the first term because the exchange constant $\alpha = 3.1 \times 10^{-12}$ cm² for YIG [30] is small. Let ζ_0 be the value of ζ calculated from the above parameters of YIG. The dispersion and the Berry curvature for $\omega_H/\omega_M = 1$ are shown in Figs. 2(a) and 2(b), and the Berry curvature for $\zeta/\zeta_0 = 0.5, 1, 2$ and $\omega_H/\omega_M = 0.5, 1, 2$ are shown in Figs. 2(c) and 2(d), respectively. These results show that the Berry curvature indeed has a strong peak at the crossing point of dispersions. The peak value of the Berry curvature in Eq. (13) for the two modes $\omega = \omega_{\pm}$ at $k = k^*$ are approximately written as

$$\Omega_{\pm,z}(k = k^*) \sim \mp \frac{1}{4k^{*2}} \frac{1}{\Delta\omega/\tilde{\omega}} \left(\frac{\Omega_0}{\tilde{\omega}} + \frac{\tilde{\omega}}{\Omega_0} \right). \quad (19)$$

Thus, the enhancement of the Berry curvature for the magnetoelastic wave is dependent on the eigenfrequencies. In addition, the Berry curvature is inversely proportional to the size of the gap $\Delta\omega$. Therefore the Berry curvature is inversely proportional to the coupling constant ζ from Eq. (16). Besides, The Berry curvature is inversely proportional to $\omega_H^{3/2}$ from Eq. (19). We illustrated the Berry curvature with several values for the coupling constant and the applied field in Figs. 2(c) and 2(d). The results in Figs. 2(c) and 2(d) indeed show the same dependencies on ζ and on ω_H with those expected from the analytical calculation.

B. Strong magnetoelastic coupling

Next, we show our calculation results for the magnetoelastic wave with strong magnetoelastic interaction in Fig. 3. While the magnetoelastic interaction in YIG is weak, in this section we set the magnetoelastic interaction to be large than its real value in order to see general behaviors of Berry curvature in the strong coupling regime. We take the same parameters as in the previous section, except for the coupling constant ζ taken of the order of $4 \times 10^2 \zeta_0$ in this section.

With this larger value of the coupling constant, the dispersion changes drastically around the crossing point at $k = k^*$. The dispersion and the Berry curvature for $\omega_H/\omega_M = 1$ are shown in Figs. 3(a) and 3(b), and the Berry curvature for $\zeta = (2, 4, 8) \times 10^2 \zeta_0$ and $\omega_H/\omega_M = 0.5, 1, 2$ are shown in Figs. 3(c) and 3(d), respectively. The hybridization gap becomes much larger and the peak value of the Berry curvature is much smaller compared with that in the previous section. In addition, the Berry curvature becomes nonzero at $k \rightarrow 0$. Particularly, the Berry curvature shown in Fig. 3(b) diverges for ω_- and remains finite for ω_+ .

Next, we analytically evaluate the Berry curvature of the magnetoelastic wave when the wave number is small: $k \ll k^*$. In particular, in the magnetoelastic wave, the magnetoelastic interaction affects even the regime $k \ll k^*$. Here we assume $\zeta^2/\omega_0^2 \gg \omega_M^2 \alpha$ and $\omega_H \sim \omega_M$. When $k \ll k^*$, $\Omega_{n,z}(k)$ read as

$$\Omega_{+,z}(k) \sim -\frac{\zeta^2}{2\omega_0^4} \frac{4 + \Lambda}{\sqrt{1 + \Lambda}}, \quad (20a)$$

for $\omega = \omega_+$ where we use $\Lambda = \omega_M/\Omega_0$, and

$$\Omega_{-,z}(k) \sim \frac{\zeta^2}{2\omega_0^4} \frac{\Omega_0}{c'k}, \quad (20b)$$

for $\omega = \omega_-$. From these results, the Berry curvature $\Omega_{-,z}(k)$ for the lower branch diverges as $1/k$ at $k \ll k^*$, while $\Omega_{+,z}(k)$ for the upper branch is finite. We note that, the Berry curvature $\Omega_{n,z}(k)$ shows a qualitatively different behavior compared with the previous result on magnons in a ferromagnetic film in the dipole-exchange regime [21], where the Berry curvature is enhanced only near the crossing point of the dispersions between the eigenmodes. Similar divergence of the Berry curvature appears in the vicinity of wave number $k \sim 0$ in systems with linear dispersion for the electromagnetic waves [14–17] and the transverse acoustic waves [37] due to the spin orbit interaction.

C. Effect of dipolar interaction

In this section, instead of the bulk ferromagnet in the previous section, we consider a ferromagnetic film and discuss the effect of the dipolar interaction on the Berry curvature of the magnetoelastic waves. In the ferromagnetic film, the form of the dipolar interaction gives nontrivial k dependence to the dispersion as is different from the bulk ferromagnet. We assume that the dipolar interaction is already saturated in the present calculation. To take into account the dipolar interaction, we start with magnons (spin waves) with dipolar interaction as has been done in Ref. [30]. We then add the magnetoelastic interaction. The resulting secular equation for the magnons with the saturated dipolar interaction is identical with that in the bulk ferromagnet (see Appendix A), while the relationship between the dipolar field and the magnetization is modified by the dipolar interaction. Therefore we replace ω_{mag} with $\omega_{\text{mag}}^2 = \Omega_0(\Omega_0 + \omega_M P_n)$, where P_n comes from the dipolar interaction and is given by [30]

$$P_n = \frac{k^2}{k^2 + \kappa_n^2} - \frac{k^4}{(k^2 + \kappa_n^2)^2} F_n \frac{1}{1 + \delta_{0n}}, \quad (21a)$$

$$F_n = \frac{2}{kL} (1 - (-1)^n \exp(-kL)). \quad (21b)$$

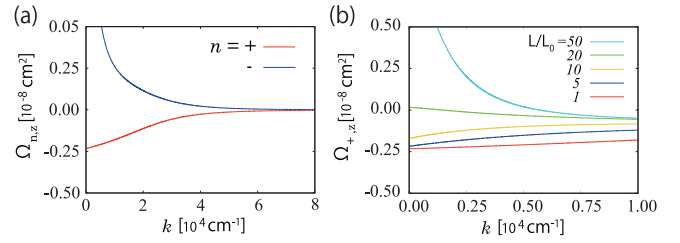


FIG. 4. Berry curvature of the magnetoelastic wave in a ferromagnetic film with dipolar interaction for $\omega_H/\omega_M = 1.0$ and $4 \times 10^2 \zeta_0$. (a) The magnetoelastic wave ω_{\pm} for $L_0 = 10^{-5}$ cm. (b) ω_+ for $L/L_0 = 1, 5, 10, 20, 50$.

Here, κ_n is the transverse wave number along the thickness direction $\kappa_n = n\pi/L$, and L is the film thickness. In the following, we only consider the $n = 0$ eigenmode with the unpinned surface spins for simplicity. The calculated Berry curvature for $\omega_H/\omega_M = 1$ and $4 \times 10^2 \zeta_0$ are shown in Figs. 4(a) and 4(b). We analyze the behavior of the Berry curvature at $k \sim 0$. In the following, we separate the Berry curvature into two parts as follows:

$$\Omega_{n,z}(k) = \Omega_{n,1}(k) + \Omega_{n,2}(k), \quad (22a)$$

where

$$\Omega_{n,1}(k) = \frac{\mathcal{R}_1}{k} \frac{\partial}{\partial k} \mathcal{R}_2, \quad (22b)$$

$$\Omega_{n,2}(k) = \frac{\mathcal{R}_2}{k} \frac{\partial}{\partial k} \mathcal{R}_1. \quad (22c)$$

$$\mathcal{R}_1 = \frac{(\omega^2 - \omega_{\text{ela}}^2)}{2(2\omega^2 - \omega_{\text{mag}}^2 - \omega_{\text{ela}}^2)}, \quad (22d)$$

$$\mathcal{R}_2 = \frac{\Omega_0}{\omega} + \frac{\omega}{\Omega_0}. \quad (22e)$$

The expression of the Berry curvature is written in Appendix B.

We first consider the Berry curvature in the absence of the magnetoelastic coupling $\zeta \rightarrow 0$. The first term of the Berry curvature in Eq. (22b) for ω_+ is written as

$$\Omega_{+,1}(k) = \frac{1}{4k} \frac{\Lambda_0}{(1 + \Lambda_0)^{3/2}} \frac{\partial \Lambda_0}{\partial k}, \quad (23)$$

where $\Lambda_0 = \omega_M P_0/\Omega_0$. This term is the same as in the previous work for the magnon with the dipolar interaction without the hybridization between eigenmodes [21]. When the magnetoelastic interaction is absent $\zeta = 0$, $\Omega_{\pm,2}$ vanishes while $\Omega_{\pm,1}$ is nonzero.

When the magnetoelastic interaction is nonzero, the Berry curvatures $\Omega_{\pm,2}$ in Eq. (22c) is no longer zero. When the dipolar interaction exists, the magnon frequency becomes $\omega_{\text{mag}} \rightarrow \omega_H$ at $k = 0$. Therefore the Berry curvature $\Omega_{+,2}$ is approximately evaluated as

$$\Omega_{+,2} \sim -\frac{2\zeta^2}{\omega_H^4}. \quad (24)$$

The Berry curvature $\Omega_{+,1}$ for the unpinned spin wave of the zeroth eigenmode becomes

$$\Omega_{+,1} \sim \left(\frac{\omega_M L}{4\omega_H} \right)^2. \quad (25)$$

from the previous works [19,21].

From these results, the Berry curvature $\Omega_{+,z} = \Omega_{+,1} + \Omega_{+,2}$ around $k \sim 0$ changes its sign from negative to positive by increasing the film thickness. This value of the film thickness is approximately given by

$$L \sim \frac{4\sqrt{2}\zeta}{\omega_M \omega_H}. \quad (26)$$

The Berry curvature $\Omega_{+,z}$ has a positive value at $k = 0$ for thick films. Then the Berry curvature $\Omega_{+,z}$ becomes negative by increasing of the wave number, as is illustrated in Fig. 4(b). For the parameter values in Fig. 4(b), the value of the film thickness at the sign change is estimated from Eq. (26) as $L \sim 19 \times 10^{-5}$ cm, which agrees with Fig. 4(b).

IV. SHIFTS OF WAVE PACKETS OF THE MAGNETOELASTIC WAVE AT A REFLECTION

In the previous section, we derived the Berry curvature for the magnetoelastic waves. One method to detect the effect of the Berry curvature is to measure a shift of a wave packet at a reflection at the edge of the magnet [21]. The shift of a wave packet due to the Berry curvature is discussed in photonic systems as well; this shift in photonic systems is called Imbert-Fedorov shift (IF shift) [14–18,38,39]. The IF shift is a transverse shift of the wave packet at a reflection or a refraction perpendicular to the incident plane. In optics, the IF shift is calculated for an interface between two isotropic media [14,15] and is compared with the result from direct calculation without the Berry curvature. Because the calculation of the shift using the Berry curvature assumes adiabatic evolution of the wave packet, i.e., a gradual interface, the result is not identical with that of the direct calculation for an abrupt interface. Nevertheless their behaviors are quite similar.

A similar shift of the wave packet at a reflection is expected for magnons as well. In the previous work [21], we calculated the shift of the magnetostatic wave induced by the Berry curvature. We can adopt the same argument in the present case of magnetoelastic waves as well. In this section, we consider the shift of a wave packet by a reflection at the edge of the ferromagnet due to the Berry curvature. The schematic figure of the shift is illustrated in Fig. 5.

A semiclassical equation of motion of the wave packet is written as

$$\dot{\mathbf{r}} = -\dot{\mathbf{k}} \times \boldsymbol{\Omega}_{n,k} + \frac{\partial \omega_n}{\partial \mathbf{k}}, \quad (27)$$

as we derive in Appendix B. This equation describes three-dimensional cases where the Berry curvature $\boldsymbol{\Omega}_n$ is a three dimensional vector. Here, we assume that the edge of the magnet is not abrupt but gradual in the scale of the wavelength. Then, the shift of the wave packet in the n th mode at the reflection is given by [21]

$$\Delta_n(\mathbf{k}) = - \int_{-\infty}^{\infty} dt \dot{\mathbf{k}} \times \boldsymbol{\Omega}_n. \quad (28)$$

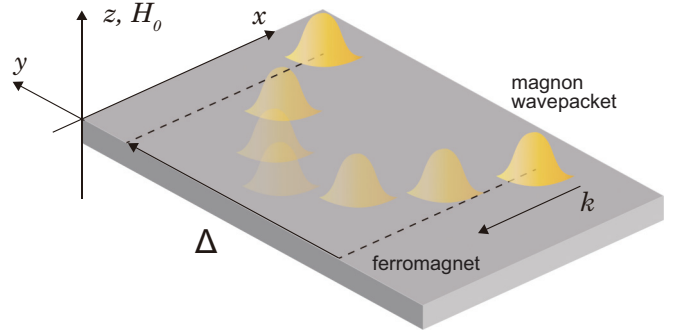


FIG. 5. Illustration of the shift of the wave packet at the interface.

In this calculation, the temporal change of the wave vector is assumed to be slow to keep the wave packet within the same eigenmode. Here, we calculate the shift of the wave packet with the weak and the strong couplings with the two coupling parameters used in Secs. III A and III B. As is similar to the previous work [21] on the magnetostatic wave, the maximum shift appears when the incident angle is zero. Therefore, we show the result of the calculation of the shift for normally incident waves.

The calculated shifts for the normally incident magnetoelastic waves for the two modes ω_{\pm} are shown in Fig. 6. The shift in the weak coupling regime [Fig. 6(a)] appears when the incident wave number k is larger than the wave number at the crossing point $k^* (\simeq 4 \times 10^4 \text{ cm}^{-1})$. The shifts of the two eigenmodes have the same sizes and the opposite signs. In contrast, the shift in the strong coupling regime [Fig. 6(b)] appears even when k is smaller than k^* . In addition, the shift for ω_- does not approach zero by decreasing k due to the divergence of Berry curvature at $k \rightarrow 0$.

Here we discuss the order of magnitude of the shift in the weak coupling regime. The width of the gap is approximately $\Delta k \sim \Delta \omega \sqrt{\rho_0/c_{44}}$. Since the width of the gap is small, the shift is approximately given by $\Delta_n(k > k^*) \sim 2\Delta k \Omega_n(k^*) \sim 1/k^*$, and the product of the shift and the wave number at the crossing point of the dispersions is constant. Therefore, the shift due to the Berry curvature with the hybridization increases by decreasing the wave number at the crossing point of the dispersions.

Here we discuss how the shift is affected by details of the edges. In fact, the shift depends on the details of the edges. When the edge is well gradual compared with the scale of the wavelength, our calculation based on the Berry curvature

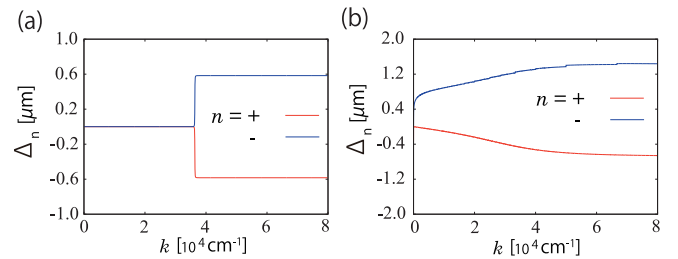


FIG. 6. Shift of the magnetoelastic wave packet at a reflection at the edge for the cases with (a) the weak coupling in Fig. 2 and with (b) the strong coupling in Fig. 3.

is justified, because the dynamics of the wave packet at the reflection is adiabatic. Meanwhile when the edge is abrupt, as in the usual boundaries between a magnet and vacuum, one can directly calculate the shift without using Berry curvature as has been done for magnetostatic waves in Refs. [40,41]. The resulting shift from such a direct calculation depends on the details of the edges.

V. CONCLUSION

In this paper, we discussed the Berry curvature for the magnetoelastic waves. For the calculation of the Berry curvature, we made the eigenvalue problem Hermitian by introducing the matrix γ . We calculated the Berry curvature of the magnetoelastic wave for $\mathbf{k} \perp \mathbf{M}_0$, and we found a peak at the anticrossing between the magnon and the elastic wave. When the wave number is small, the Berry curvature diverges toward $k \rightarrow 0$ for the lower branch, and this divergence is prominent when the magnetoelastic coupling is strong. Meanwhile, the Berry curvature for the upper branch converges to a finite value at $k \rightarrow 0$. Besides, we also calculated the Berry curvature of the magnetoelastic waves at $k \rightarrow 0$ with the dipolar interaction. The Berry curvature changes its sign by changing the film thickness. We also calculated the shift of the wave packet of the magnetoelastic wave at the reflection at the gradual edge. The behavior of the shift is characterized by the strength of the hybridization. When the magnetoelastic interaction is small, the size of the shift is dependent on whether the wave number of the incident wave k is larger or smaller than the wave number at the crossing point k^* , and its size is approximately inversely proportional to k^* .

ACKNOWLEDGMENTS

We are grateful to M. Hamada for fruitful discussions. This work was supported by MEXT KAKENHI Grant Number JP26103006, Japan, and KES is funded by the German Research Foundation (DFG) under the Project No. EV 196/2-1.

APPENDIX A: DYNAMICAL EQUATION OF MOTION FOR MAGNETOELASTIC WAVES

In this Appendix, we derive a dynamical equation of motion of magnons and elastic waves with the magnetoelastic interaction. In order to calculate the Berry curvature, we consider the dynamical equation with an arbitrary angle between the saturation magnetization and the wave vector. Here, we consider a bulk ferromagnet with the saturation magnetization \mathbf{M}_0 and the applied magnetic field \mathbf{H}_0 , both along the z direction. Then the magnon is described by a vector \mathbf{m} in the xy plane. In the following, we assume the system to be elastically isotropic and we neglect dissipation in the system. The equation of motion for the elastic wave is given by [29,34] ($i, j, k, l = 1, 2, 3$)

$$\rho_0 \frac{\partial^2 u_i}{\partial t^2} = \sum_j \sum_l \sum_m c_{ijlm} \frac{\partial^2 u_m}{\partial x_j \partial x_l} \quad (\text{A1})$$

where u_i is the i th component of the displacement vector and ρ_0 is the equilibrium mass density. c_{ijkl} is the elastic moduli

written as

$$c_{ijkl} = \frac{\partial \sigma_{ik}}{\partial \gamma_{lm}}, \quad (\text{A2})$$

where σ_{ik} is the stress tensor, and γ_{ik} is the deformation tensor written as

$$\gamma_{ik} = \frac{1}{2} \left(\frac{\partial u_i}{\partial x_k} + \frac{\partial u_k}{\partial x_i} \right). \quad (\text{A3})$$

We use the following notation: $c_{iii} \equiv c_{11}$, $c_{ijij} \equiv c_{12}$, and $c_{ijij} \equiv c_{44}$. The relation $c_{11} - c_{12} = 2c_{44}$ holds for an isotropic media.

Next, we consider an effective field \mathbf{H}_{eff} which is a sum of the magnetic field and the dipolar field \mathbf{h}_d . The dipolar field is determined by the following formulas:

$$\nabla \times \mathbf{h}_d = \mathbf{0}, \quad \nabla \cdot (\mathbf{h}_d + \mathbf{m}) = 0. \quad (\text{A4})$$

Here we set \mathbf{h}_d to be proportional to $\exp i(\mathbf{k} \cdot \mathbf{r} - \omega t)$. Then, from the first equation, the dipolar field is written as $\mathbf{h}_d = \hat{\mathbf{k}} h_d$ where $\hat{\mathbf{k}} = \mathbf{k}/k$. Substituting this result into the second equation of Eqs. (A4), we obtain

$$h_d = -\hat{\mathbf{k}} \cdot \mathbf{m}. \quad (\text{A5})$$

Substituting this result for the dipolar field \mathbf{h}_d into the dynamical equation with the magnetoelastic interaction [3,29], we obtain the equation of motion for the magnetoelastic waves:

$$-i\omega m_x = -\Omega_0 m_y + \omega_M h_{d,y} - igB_2(k_y u_z + k_z u_y), \quad (\text{A6a})$$

$$-i\omega m_y = \Omega_0 m_x - \omega_M h_{d,x} + igB_2(k_x u_z + k_z u_x), \quad (\text{A6b})$$

$$-\rho_0 \omega^2 u_x = -c_{44} k^2 u_x - (c_{44} + c_{12}) k_x \mathbf{k} \cdot \mathbf{u} + i \frac{gB_2}{\omega_M} k_z m_x, \quad (\text{A6c})$$

$$-\rho_0 \omega^2 u_y = -c_{44} k^2 u_y - (c_{44} + c_{12}) k_y \mathbf{k} \cdot \mathbf{u} + i \frac{gB_2}{\omega_M} k_z m_y, \quad (\text{A6d})$$

$$-\rho_0 \omega^2 u_z = -c_{44} k^2 u_z - (c_{44} + c_{12}) k_z \mathbf{k} \cdot \mathbf{u} + i \frac{gB_2}{\omega_M} (k_x m_x + k_y m_y). \quad (\text{A6e})$$

where $\omega_M = gM_0$, g is the gyromagnetic ratio, and B_2 is a magnetoelastic coupling constant. Ω_0 includes only the Zeeman energy and the exchange interaction in the form as $\Omega_0 = \omega_H + \omega_M \alpha k^2$, $\omega_H = gH_0$ and α is the exchange constant as in Ref. [30].

In Sec. II, we consider the case where the wave vector is perpendicular to the magnetization. In this Appendix A, we instead study the case when the wave vector is parallel to the magnetization. Then the dipole field is absent in the system [28]. The equation of motion is written as

$$-i\omega m_x = -\Omega_0 m_y - igB_2 k u_y, \quad (\text{A7a})$$

$$-i\omega m_y = \Omega_0 m_x + igB_2 k u_x, \quad (\text{A7b})$$

$$-\rho_0 \omega^2 u_x = -c_{44} k^2 u_x + i \frac{gB_2}{\omega_M} k m_x, \quad (\text{A7c})$$

$$-\rho_0 \omega^2 u_y = -c_{44} k^2 u_y + i \frac{gB_2}{\omega_M} k m_y, \quad (\text{A7d})$$

$$-\rho_0 \omega^2 u_z = -(2c_{44} + c_{12}) k^2 u_z. \quad (\text{A7e})$$

The magnon \mathbf{m} and the transverse elastic wave of u_x , u_y are coupled with each other while the longitudinal elastic wave u_z is decoupled. When we take the eigenvector to be $\mathbf{x}_k = {}^t(m_x, m_y, \dot{u}_x, \dot{u}_y, u_x, u_y)$, the effective 6×6 Hamiltonian matrix reads as

$$H_{\text{eff}}^{\parallel} = \begin{pmatrix} \Omega_0 \sigma_y & \mathbf{0} & igB_2 k \sigma_2 \\ -\frac{gB_2}{\rho_0 \omega_M} k I_2 & \mathbf{0} & -ic_{44} k^2 / \rho_0 I_2 \\ \mathbf{0} & iI_2 & \mathbf{0} \end{pmatrix}, \quad (\text{A8})$$

where I_2 is the 2×2 unit matrix, $\mathbf{0}$ is the 2×2 zero matrix and σ_y is the 2×2 Pauli matrix. From this effective Hamiltonian, we can derive the matrix γ^{\parallel} by the same approach with that the main text:

$$\gamma^{\parallel} = \begin{pmatrix} \sigma_y & \mathbf{0} & \mathbf{0} \\ \mathbf{0} & \mathbf{0} & -i\rho_0 \omega_M I_2 \\ \mathbf{0} & i\rho_0 \omega_M I_2 & \mathbf{0} \end{pmatrix}, \quad (\text{A9})$$

which makes the effective Hamiltonian to be Hermitian as

$$\tilde{H}_{\text{eff}}^{\parallel} = \gamma^{\parallel} H_{\text{eff}}^{\parallel} = \begin{pmatrix} \Omega_0 I_2 & \mathbf{0} & igB_2 k I_2 \\ \mathbf{0} & \rho_0 \omega_M I_2 & 0 \\ -igB_2 k I_2 & \mathbf{0} & \omega_M c_{44} k^2 I_2 \end{pmatrix}. \quad (\text{A10})$$

From this Hamiltonian, we obtain dispersion relations:

$$\left[(\omega + \Omega_0)(\omega^2 - \omega_{\text{ela}}^2) + \frac{g^2 B_2^2 k^2}{\rho_0 \omega_M} \right] \times \left[(\omega - \Omega_0)(\omega^2 - \omega_{\text{ela}}^2) - \frac{g^2 B_2^2 k^2}{\rho_0 \omega_M} \right] = 0. \quad (\text{A11})$$

$$\tilde{H}_{\text{eff},k} = \gamma H_{\text{eff}}(k, \varphi) = \begin{pmatrix} \Omega_0 + \omega_M \cos^2 \varphi & \omega_M \sin \varphi \cos \varphi & 0 & igB_2 k \cos \varphi \\ \omega_M \sin \varphi \cos \varphi & \Omega_0 + \omega_M \sin^2 \varphi & 0 & igB_2 k \sin \varphi \\ 0 & 0 & \omega_M \rho_0 & 0 \\ -igB_2 k \cos \varphi & -igB_2 k \sin \varphi & 0 & \omega_M c_{44} k^2 \end{pmatrix}, \quad (\text{B2})$$

where φ is the angle between the x axis and the wave vector, and

$$\gamma = \begin{pmatrix} 0 & -i & 0 & 0 \\ i & 0 & 0 & 0 \\ 0 & 0 & 0 & -i\rho_0 \omega_M \\ 0 & 0 & i\rho_0 \omega_M & 0 \end{pmatrix}, \quad (\text{B3})$$

$$\mathbf{x}_k = \begin{pmatrix} m_{x,k} \\ m_{y,k} \\ \dot{u}_{z,k} \\ u_{z,k} \end{pmatrix}. \quad (\text{B4})$$

By using the properties of the matrices $\tilde{H}_{\text{eff},k}$ and γ ,

$$\gamma^* = -\gamma, \quad (\text{B5})$$

$$\tilde{H}_{\text{eff},-k}^* = \tilde{H}_{\text{eff},k}, \quad (\text{B6})$$

This result is identical with the results in Refs. [3,27,29]. As is expected, the norm of the eigenvector $\mathbf{x}_k^{\dagger} \gamma^{\parallel} \mathbf{x}_k$ is proportional to the energy density of the magnon and the elastic wave.

APPENDIX B: DERIVATION OF THE SEMICLASSICAL EQUATION OF MOTION AND THE BERRY CURVATURE FOR THE MAGNETOELASTIC WAVE

In this Appendix, we derive the Berry curvature of the magnetoelastic wave used in this article by formulating the semiclassical equation of motion. This follows the same approach as we used in Ref. [30]. First, we consider orthogonality and completeness relations from the Hermitian eigenvalue equation to calculate the Wannier function. Next, we calculate the propagator of the Bloch wave function from the initial state to the final state, and derive the semiclassical equation of motion in the coupled waves. From this equation of motion, we can read off the formula of the Berry curvature of the magnetoelastic wave in the classical problem (1). In the following calculation, we use the Hermitian eigenvalue equation when the wave vector \mathbf{k} is perpendicular to the saturation magnetization \mathbf{M}_0 and in the xy plane. In such a case, the elastic waves of u_x and u_y are decoupled from other degrees of freedom, and we only consider the coupled waves with m_x , m_y , and u_z .

In order to show the orthogonality and completeness relations, we introduce the eigenstates for positive and negative eigenvalues. The eigenvalue problem is rewritten as the following form:

$$\tilde{H}_{\text{eff},k} \mathbf{x}_{j,k} = \omega_{jk} \gamma \mathbf{x}_{j,k}, \quad (\text{B1})$$

where j is the index of the eigenmodes for the magnetoelastic waves. The matrix $\tilde{H}_{\text{eff},k}$ for $\mathbf{k} \perp \mathbf{M}_0$ is given by

we obtain

$$\tilde{H}_{\text{eff},k} \bar{\mathbf{x}}_{j,k} = -\omega_{j,-k} \gamma \bar{\mathbf{x}}_{j,k}, \quad (\text{B7})$$

where $\bar{\mathbf{x}}_{j,k}$ is defined as $\bar{\mathbf{x}}_{j,k} = \mathbf{x}_{j,-k}^*$. Thus, if $\mathbf{x}_{j,k}$ describes an eigenmode with a positive frequency, $\bar{\mathbf{x}}_{j,k}$ describes that with a negative frequency, and vice versa. Then orthogonality and completeness relations of eigenvectors are written as

$$\mathbf{x}_{i,k}^{\dagger} \gamma \mathbf{x}_{j,k} = \delta_{ij}, \quad (\text{B8a})$$

$$\bar{\mathbf{x}}_{i,k}^{\dagger} \gamma \bar{\mathbf{x}}_{j,k} = -\delta_{ij}, \quad (\text{B8b})$$

$$\bar{\mathbf{x}}_{i,k}^{\dagger} \gamma \mathbf{x}_{j,k} = 0 = \mathbf{x}_{i,k}^{\dagger} \gamma \bar{\mathbf{x}}_{j,k}, \quad (\text{B8c})$$

and

$$\sum_{j=1}^N (\mathbf{x}_{j,k} \mathbf{x}_{j,k}^{\dagger} - \bar{\mathbf{x}}_{j,k} \bar{\mathbf{x}}_{j,k}^{\dagger}) = \gamma^{-1}. \quad (\text{B8d})$$

where N is the number of eigenmodes with a positive frequency.

In terms of these eigenvectors, the Bloch wave functions are written as

$$\psi_{j,k}(\mathbf{r}) = e^{i\mathbf{k}\cdot\mathbf{r}}\mathbf{x}_{j,k}(\mathbf{r}), \quad (\text{B9a})$$

$$\bar{\psi}_{j,k}(\mathbf{r}) = e^{i\mathbf{k}\cdot\mathbf{r}}\bar{\mathbf{x}}_{j,k}(\mathbf{r}). \quad (\text{B9b})$$

Then we get

$$\begin{aligned} \langle\langle\mathbf{r}|\hat{\mathbf{r}}|\psi_{j,k}\rangle\rangle &= \mathbf{r}\langle\langle\mathbf{r}|\psi_{j,k}\rangle\rangle \\ &= -i\frac{\partial\psi_{j,k}}{\partial\mathbf{k}} + ie^{i\mathbf{k}\cdot\mathbf{r}}\frac{\partial\mathbf{x}_{j,k}}{\partial\mathbf{k}} \\ &= -i\frac{\partial\psi_{j,k}}{\partial\mathbf{k}} + ie^{i\mathbf{k}\cdot\mathbf{r}}\sum_{i=1}^N(\mathbf{x}_{i,k}\mathbf{x}_{i,k}^\dagger - \bar{\mathbf{x}}_{i,k}\bar{\mathbf{x}}_{i,k}^\dagger)\gamma\frac{\partial\mathbf{x}_{j,k}}{\partial\mathbf{k}}, \end{aligned} \quad (\text{B10})$$

where $\hat{\mathbf{r}}$ is the position operator, and we use the notation $|\dots\rangle$ to represent a wave function defined in real space with the coordinate $\mathbf{r} = (x, y)$. We can construct the Wannier functions $w_{j,r}$ and $\bar{w}_{j,r}$ associated with the Bloch wave functions $\psi_{j,k}$ and $\bar{\psi}_{j,k}$, respectively. Then we approximately obtain

$$\hat{\mathbf{r}}|w_{j,r}\rangle = \mathbf{r}|w_{j,r}\rangle, \quad \hat{\mathbf{r}}|\bar{w}_{j,r}\rangle = \mathbf{r}|\bar{w}_{j,r}\rangle. \quad (\text{B11})$$

From this equation, we get

$$\langle\langle\psi_{j,k}|\gamma\hat{\mathbf{r}}|w_{j,r}\rangle\rangle = \langle\langle\psi_{j,k}|\gamma\mathbf{r}|w_{j,r}\rangle\rangle. \quad (\text{B12})$$

We adopt a ‘‘single-band approximation’’ into Eq. (B10), by retaining only the $\mathbf{x}_{j,k}\mathbf{x}_{j,k}^\dagger$ term in the summation in Eq. (B10). Then we obtain

$$\left(\mathbf{r} - i\frac{\partial}{\partial\mathbf{k}} - \mathbf{\Lambda}_{j,k}\right)\langle\langle\psi_{j,k}|\gamma|w_{j,r}\rangle\rangle = 0, \quad (\text{B13})$$

where $\mathbf{\Lambda}_{j,k}$ is the Berry connection in \mathbf{k} space

$$\mathbf{\Lambda}_{j,k} = i\mathbf{x}_{j,k}^\dagger\gamma\frac{\partial\mathbf{x}_{j,k}}{\partial\mathbf{k}} \quad (\text{B14})$$

From Eq. (B13), the term $\langle\langle\psi_{j,k}|\gamma|w_{j,r}\rangle\rangle$ can be written as

$$\langle\langle\psi_{j,k}|\gamma|w_{j,r}\rangle\rangle = \exp\left(-i\mathbf{k}\cdot\mathbf{r} + i\int_{\mathbf{k}_0}^{\mathbf{k}}\mathbf{\Lambda}_{j,k}\cdot d\mathbf{k}\right). \quad (\text{B15})$$

The completeness property of the Bloch wave function and the Wannier function are expressed as

$$\int\frac{d^2k}{2\pi}\sum_{j=1}^N(|\psi_{j,k}\rangle\rangle\langle\langle\psi_{j,k}| - |\bar{\psi}_{j,k}\rangle\rangle\langle\langle\bar{\psi}_{j,k}|) = \gamma^{-1} \quad (\text{B16a})$$

and

$$\int\frac{d^2r}{2\pi}\sum_{j=1}^N(|w_{j,r}\rangle\rangle\langle\langle w_{j,r}| - |\bar{w}_{j,r}\rangle\rangle\langle\langle\bar{w}_{j,r}|) = \gamma^{-1}. \quad (\text{B16b})$$

Next, we calculate a propagator of the Bloch wave $\langle\langle\psi_{n,k_i}|\gamma\exp(-i\hat{H}(t_f - t_i))|\psi_{n,k_j}\rangle\rangle$, where $\hat{H} = e^{i\mathbf{k}\cdot\mathbf{r}}H_{\mathbf{k}}e^{-i\mathbf{k}\cdot\mathbf{r}}$.

Here we calculate a propagator for a short interval of time ϵ .

$$\begin{aligned} &\langle\langle\psi_{n,k_{j+1}}|\gamma\exp(-i\hat{H}\epsilon)|\psi_{n,k_j}\rangle\rangle \\ &= \int\frac{d^2r}{2\pi}\langle\langle\psi_{n,k_{j+1}}|\gamma|w_{nr}\rangle\rangle\langle\langle w_{nr}|\gamma\exp(-i\hat{H}\epsilon)|\psi_{n,k_j}\rangle\rangle \\ &= \int\frac{d^2r}{2\pi}\exp\left[i\epsilon\left(-\mathbf{r}\cdot\frac{\mathbf{k}_{j+1}-\mathbf{k}_j}{\epsilon} + \mathbf{\Lambda}_{n,k}\cdot\frac{\mathbf{k}_{j+1}-\mathbf{k}_j}{\epsilon} - \omega_{n,k}\right)\right], \end{aligned} \quad (\text{B17})$$

where we used the completeness property of the Wannier functions, Eq. (B16b). Finally, the propagator is expressed as

$$\begin{aligned} &\langle\langle\psi_{n,k_i}|\gamma e^{(-i\hat{H}(t_f - t_i))}|\psi_{n,k_j}\rangle\rangle \\ &= \int\mathcal{D}(\mathbf{k})\mathcal{D}(\mathbf{r})\exp\left(i\int_{t_i}^{t_f}\mathcal{L}_k dt\right), \end{aligned} \quad (\text{B18})$$

with the Lagrangian given by \mathcal{L}_k

$$\mathcal{L}_k = -\mathbf{r}\cdot\dot{\mathbf{k}} + \mathbf{\Lambda}_{n,k}\cdot\dot{\mathbf{k}} - \omega_{n,k}. \quad (\text{B19})$$

By using the variational principle, we obtain the semiclassical equation of motion

$$\dot{\mathbf{r}} = -\dot{\mathbf{k}}\times\mathbf{\Omega}_{n,k} + \frac{\partial\omega_{n,k}}{\partial\mathbf{k}}, \quad (\text{B20})$$

where the Berry curvature $\mathbf{\Omega}_{n,k}$ is given in the form identical with Eq. (13). We note that the Berry curvature is gauge invariant under the gauge transformation $\mathbf{x}_k \Rightarrow \tilde{\mathbf{x}}_k = e^{i\Theta_k}\mathbf{x}_k$ (Θ_k : real). Indeed, the Berry curvature is transformed as

$$\begin{aligned} \Omega_{n,z}(\mathbf{k}) &\Rightarrow i\epsilon_{ij}\frac{\partial\tilde{\mathbf{x}}_{n,k}^\dagger}{\partial k_i}\gamma\frac{\partial\tilde{\mathbf{x}}_{n,k}}{\partial k_j} \\ &= i\epsilon_{ij}\left[\mathbf{x}_{n,k}^\dagger\frac{\partial\Theta_k}{\partial k_i}\gamma\frac{\partial\Theta_k}{\partial k_j}\mathbf{x}_{n,k} + \frac{\partial\mathbf{x}_{n,k}^\dagger}{\partial k_i}\gamma\frac{\partial\mathbf{x}_{n,k}}{\partial k_j} \right. \\ &\quad \left. + i\frac{\partial\mathbf{x}_{n,k}^\dagger}{\partial k_i}\gamma\frac{\partial\Theta_k}{\partial k_j}\mathbf{x}_{n,k} - i\mathbf{x}_{n,k}^\dagger\frac{\partial\Theta_k}{\partial k_i}\gamma\frac{\partial\mathbf{x}_{n,k}}{\partial k_j}\right] \\ &= i\epsilon_{ij}\frac{\partial\mathbf{x}_{n,k}^\dagger}{\partial k_i}\gamma\frac{\partial\mathbf{x}_{n,k}}{\partial k_j} = \Omega_{n,z}(\mathbf{k}), \end{aligned} \quad (\text{B21})$$

where we use the relation $\frac{\partial\mathbf{x}_k^\dagger}{\partial k_i}\gamma\mathbf{x}_k = -\mathbf{x}_k^\dagger\gamma\frac{\partial\mathbf{x}_k}{\partial k_i}$.

The Berry curvature of the magnetoelastic wave for $\mathbf{k}\perp\mathbf{M}_0$ is easily calculated. Equation (B2) with an arbitrary value of φ can be reduced to that with $\varphi = 0$

$$\tilde{H}_{\text{eff}}(k, \varphi = 0)\tilde{\mathbf{x}}_k = \omega\gamma\tilde{\mathbf{x}}_k, \quad (\text{B22})$$

by the following transformation:

$$\mathbf{x}_k = \begin{pmatrix} U_2(\varphi) & \mathbf{0} & \mathbf{0} \\ \mathbf{0} & 1 & 0 \\ \mathbf{0} & 0 & 1 \end{pmatrix}\tilde{\mathbf{x}}_k, \quad U_2(\varphi) = \begin{pmatrix} \cos\varphi & -\sin\varphi \\ \sin\varphi & \cos\varphi \end{pmatrix}, \quad (\text{B23})$$

where we omitted the subscript j . It reflects the fact that the value of φ does not affect the setup when $\mathbf{k}\perp\mathbf{M}_0$. When

$\varphi = 0$, the matrix H is largely simplified as

$$\tilde{H}_{\text{eff}}(k, \varphi = 0) = \begin{pmatrix} \Omega_0 + \omega_M & 0 & 0 & igB_2k \\ 0 & \Omega_0 & 0 & 0 \\ 0 & 0 & \rho_0\omega_M & 0 \\ -igB_2k & 0 & 0 & \omega_M c_{44}k^2 \end{pmatrix}. \quad (\text{B24})$$

Namely, the dependence on k and φ is separated. Then the Berry curvature is calculated as

$$\begin{aligned} \Omega_{n,z}(\mathbf{k}) &= i\epsilon_{\alpha\beta} \frac{\partial \mathbf{x}_k^\dagger}{\partial k_\alpha} \gamma \frac{\partial \mathbf{x}_k}{\partial k_\beta} \\ &= \frac{1}{k} \frac{\partial}{\partial k} (\tilde{\mathbf{x}}_k^\dagger \Gamma \tilde{\mathbf{x}}_k), \end{aligned} \quad (\text{B25})$$

$$\Gamma = \begin{pmatrix} 1 & 0 & 0 & 0 \\ 0 & 1 & 0 & 0 \\ 0 & 0 & 0 & 0 \\ 0 & 0 & 0 & 0 \end{pmatrix}, \quad (\text{B26})$$

with the normalization condition $\tilde{\mathbf{x}}_k^\dagger \gamma \tilde{\mathbf{x}}_k = 1$. Furthermore, it is sometimes convenient to use an unnormalized eigenstate $\tilde{\mathbf{X}}_k$ ($\propto \tilde{\mathbf{x}}_k$):

$$\Omega_{n,z}(\mathbf{k}) = \frac{1}{k} \frac{\partial}{\partial k} \left(\frac{\tilde{\mathbf{X}}_k^\dagger \Gamma \tilde{\mathbf{X}}_k}{\tilde{\mathbf{X}}_k^\dagger \gamma \tilde{\mathbf{X}}_k} \right), \quad (\text{B27})$$

where $\tilde{\mathbf{X}}_k$ is an unnormalized wave function for \mathbf{x}_k .

Next we calculate the Berry curvature for the magnetoelastic wave. From the Hermitian eigenvalue equation

$$\begin{pmatrix} \Omega_0 + \omega_M & i\omega & 0 & igB_2k \\ -i\omega & \Omega_0 & 0 & 0 \\ 0 & 0 & \rho_0\omega_M & i\rho_0\omega_M\omega \\ -igB_2k & 0 & -i\rho_0\omega_M\omega & \omega_M c_{44}k^2 \end{pmatrix} \tilde{\mathbf{X}}_k = \mathbf{0}, \quad (\text{B28})$$

we obtain the wave function $\tilde{\mathbf{X}}_k$ as

$$\tilde{\mathbf{X}}_k = \begin{pmatrix} ig\Omega_0 B_2k \\ -g\omega B_2k \\ -i\omega(\omega^2 - \omega_{\text{mag}}^2) \\ \omega^2 - \omega_{\text{mag}}^2 \end{pmatrix}, \quad (\text{B29})$$

and the eigenfrequency ω :

$$\omega_{\pm}^2 = \frac{\omega_{\text{mag}}^2 + \omega_{\text{ela}}^2}{2} \pm \frac{1}{2} \sqrt{(\omega_{\text{mag}}^2 - \omega_{\text{ela}}^2)^2 + 4(\zeta k)^2}. \quad (\text{B30})$$

Finally, from Eq. (B27), we obtain the Berry curvature:

$$\Omega_{\pm,z}(\mathbf{k}) = \frac{1}{k} \frac{\partial}{\partial k} \left(\frac{(\omega_{\pm}^2 - \omega_{\text{ela}}^2)(\frac{\Omega_0}{\omega_{\pm}} + \frac{\omega_{\pm}}{\Omega_0})}{2(2\omega_{\pm}^2 - \omega_{\text{mag}}^2 - \omega_{\text{ela}}^2)} \right), \quad (\text{B31})$$

which gives Eqs. (22b) and (22c) in Sec. III C in the main text.

APPENDIX C: WAVE NUMBER AND BERRY CURVATURE AT THE CROSSING POINT OF THE DISPERSIONS OF THE MAGNON AND THE ELASTIC WAVE

Here we present details about the wave number k^* at the crossing point between the dispersions of magnons and the elastic waves. Their dispersions cross when $\omega_{\text{mag}} = \omega_{\text{ela}}$, i.e.

$$\frac{c_{44}}{\rho_0} k^{*2} = \Omega_0(\Omega_0 + \omega_M). \quad (\text{C1})$$

We can obtain the wave number at the crossing as

$$k^* = \sqrt{\frac{\rho_0}{c_{44}} \Omega_0(\Omega_0 + \omega_M)}. \quad (\text{C2})$$

By using the formulas

$$\omega_{\text{mag}}^2 = \frac{c_{44}}{\rho_0} k^{*2} = \tilde{\omega}^2, \quad \omega_{\text{ela}}^2 = \frac{c_{44}}{\rho_0} k^2, \quad (\text{C3})$$

we obtain the frequencies of the eigenmodes

$$\begin{aligned} \omega &\sim \sqrt{\frac{c_{44}(k^2 + k^{*2})}{2\rho_0}} \\ &\times \left(1 \pm \frac{1}{4(k^2 + k^{*2})} \sqrt{\frac{(k^{*2} - k^2)^2}{4} + \left(\frac{\rho_0 \zeta k}{c_{44}}\right)^2} \right). \end{aligned} \quad (\text{C4})$$

Therefore, the peak value of the Berry curvature for the two modes $\omega = \omega_{\pm}$ in Eq. (B31) at $k = k^*$ are approximately written as

$$\begin{aligned} \Omega_{\pm,z}(k = k^*) &\sim \mp \frac{c_{44}}{4\rho_0 \zeta k^*} \left(\frac{\Omega_0}{\tilde{\omega}} + \frac{\tilde{\omega}}{\Omega_0} \right) \\ &\sim \mp \frac{1}{4k^{*2}} \frac{1}{\Delta\omega/\tilde{\omega}} \left(\frac{\Omega_0}{\tilde{\omega}} + \frac{\tilde{\omega}}{\Omega_0} \right), \end{aligned} \quad (\text{C5})$$

which gives Eq. (19) in the main text.

-
- [1] C. Kittel, *Phys. Rev.* **110**, 836 (1958).
[2] A. I. Akhiezer, V. G. Bar'yakhtar, and S. V. Peletminskii, *Zh. Eksp. Teor. Fiz.* **35**, 228 (1958). [*Sov. Phys. JETP* **8**, 157 (1959)].
[3] E. Schlömann, *J. Appl. Phys.* **31**, 1647 (1960).
[4] J. R. Eshbach, *Phys. Rev. Lett.* **8**, 357 (1962).
[5] J. R. Eshbach, *J. Appl. Phys.* **34**, 1298 (1963).
[6] W. Strauss, *Proc. IEEE* **53**, 1485 (1965).
[7] W. Strauss, *J. Appl. Phys.* **36**, 118 (1965).
[8] Y. Hashimoto, S. Daimon, R. Iguchi, Y. Oikawa, K. Shen, K. Sato, D. Bossini, Y. Tabuchi, T. Satoh, B. Hillebrands, G. E. W. Bauer, T. H. Johansen, A. Kirilyuk, T. Rasing, and E. Saitoh, *Nat. Commun.* **8**, 15859 (2017).
[9] K. Shen and G. E. W. Bauer, *Phys. Rev. Lett.* **115**, 197201 (2015).
[10] A. Kamra and G. E. W. Bauer, *Solid State Commun.* **198**, 35 (2014).
[11] A. Kamra, H. Keshtgar, P. Yan, and G. E. W. Bauer, *Phys. Rev. B* **91**, 104409 (2015).
[12] T. Kikkawa, K. Shen, B. Flebus, R. A. Duine, K.-i. Uchida, Z. Qiu, G. E. W. Bauer, and E. Saitoh, *Phys. Rev. Lett.* **117**, 207203 (2016).
[13] D. A. Bozhko, P. Clausen, A. V. Chumak, Y. V. Kobljanskyj, B. Hillebrands, and A. A. Serga, *Low Temp. Phys.* **41**, 801 (2015).
[14] M. Onoda, S. Murakami, and N. Nagaosa, *Phys. Rev. Lett.* **93**, 083901 (2004).

- [15] M. Onoda, S. Murakami, and N. Nagaosa, *Phys. Rev. E* **74**, 066610 (2006).
- [16] K. Y. Bliokh and Y. P. Bliokh, *Phys. Rev. E* **70**, 026605 (2004).
- [17] K. Y. Bliokh and V. D. Freilikher, *Phys. Rev. B* **72**, 035108 (2005).
- [18] K. Y. Bliokh and Y. P. Bliokh, *Phys. Rev. Lett.* **96**, 073903 (2006).
- [19] R. Matsumoto and S. Murakami, *Phys. Rev. B* **84**, 184406 (2011).
- [20] R. Matsumoto and S. Murakami, *Phys. Rev. Lett.* **106**, 197202 (2011).
- [21] A. Okamoto and S. Murakami, *Phys. Rev. B* **96**, 174437 (2017).
- [22] E. Thingstad, A. Kamra, A. Brataas, and A. Sudbø, *Phys. Rev. Lett.* **122**, 107201 (2019).
- [23] X. Zhang, Y. Zhang, S. Okamoto, and D. Xiao, *Phys. Rev. Lett.* **123**, 167202 (2019).
- [24] L. Zhang, J. Ren, J.-S. Wang, and B. Li, *Phys. Rev. Lett.* **105**, 225901 (2010).
- [25] L. Zhang, J. Ren, J.-S. Wang, and B. Li, *J. Phys. Condens. Matter* **23**, 305402 (2011).
- [26] T. Qin, J. Zhou, and J. Shi, *Phys. Rev. B* **86**, 104305 (2012).
- [27] A. I. Akhiezer, V. G. Bar'yakhtar, and S. V. Peletminskii, *Spin Waves* (North-Holland, Amsterdam, 1968).
- [28] V. G. Bar'yakhtar and E. A. Turov, in *Spin Waves and Magnetic Excitations*, edited by A. S. Borovik-Romanov and S. K. Sinha (North-Holland, Amsterdam, 1988).
- [29] A. G. Gurevich and G. A. Melkov, *Magnetization Oscillations and Waves* (CRC Press, Boca Raton, 1996).
- [30] B. A. Kalinikos and A. N. Slavin, *J. Phys. C* **19**, 7013 (1986).
- [31] D. A. Fishman and F. R. Morgenthaler, *J. Appl. Phys.* **54**, 3387 (1983).
- [32] N. E. Buris and D. D. Stancil, *IEEE Trans. Microwave Theory Tech.* **33**, 484 (1985).
- [33] F. Morgenthaler, *IEEE Trans. Magn.* **8**, 130 (1972).
- [34] F. I. Fedorov, *Theory of Elastic Waves in Crystals* (Plenum, New York, 1968).
- [35] A. Rückriegel, P. Kopietz, D. A. Bozhko, A. A. Serga, and B. Hillebrands, *Phys. Rev. B* **89**, 184413 (2014).
- [36] I. K. Kikoin, *Tables of Physical Quantities* (Atomizdat, Moscow, 1976).
- [37] K. Y. Bliokh and V. D. Freilikher, *Phys. Rev. B* **74**, 174302 (2006).
- [38] C. Imbert, *Phys. Rev. D* **5**, 787 (1972).
- [39] O. Hosten and P. Kwiat, *Science* **319**, 787 (2008).
- [40] Y. S. Dadoenkova, N. N. Dadoenkova, I. L. Lyubchanskii, M. L. Sokolovskyy, J. W. Klos, J. Romero-Vivas, and M. Krawczyk, *Appl. Phys. Lett.* **101**, 042404 (2012).
- [41] P. Gruszecki, J. Romero-Vivas, Y. S. Dadoenkova, N. N. Dadoenkova, I. L. Lyubchanskii, and M. Krawczyk, *Appl. Phys. Lett.* **105**, 242406 (2014).